Electromagnetically induced conical emission

E. M. Becerra-Castro and Luís E. E. de Araujo*
Instituto de Física "Gleb Wataghin," Universidade Estadual de Campinas, Campinas - SP, 13083-970, Brazil
(Received 8 September 2010; published 23 December 2010)

We describe theoretically a scheme for observing conical emission, a transverse nonlinear optical effect, in an atomic vapor with all excitation fields below the saturation level of the involved atomic transitions. The scheme relies on the giant Kerr nonlinearities possible under electromagnetically induced transparency to introduce a radially varying phase shift to a weak probe field by a weak signal field. The probe's far-field diffraction pattern shows multiple concentric rings around the probe beam's axis, characteristic of conical emission.

DOI: 10.1103/PhysRevA.82.065802 PACS number(s): 42.50.Gy, 42.65.−k

Kerr-type optical nonlinearities play a key role in the field of nonlinear optics [1]. Usually, Kerr nonlinearities are rather low because large detunings, which weaken the nonlinearity, are necessary to avoid absorption. Therefore, practical nonlinear effects require intense optical fields, even in atomic vapors, which can exhibit a large nonlinear response close to an atomic resonance. When an intense light beam propagates through a nonlinear medium, transverse effects, which change the beam spatial profile, can be observed. Conical emission (CE) is one such nonlinear transverse effect, and it has been the subject of extensive study [2]. CE is characterized by the formation of a ring pattern around the original beam. It has been observed in atomic vapors, glasses, liquid-crystal films, and other materials. CE can originate from the Kerr nonlinear effects of self-phase modulation [3–5] and cross phase modulation (XPM) [6]. However, several other physical mechanisms have also been proposed to explain CE, including Cerenkov-like emission [7], the cooperative effect [8], and four-wave mixing [9], among various others [2]. Typically, experimental CE observations have been made with pulsed laser intensities greater than 10^6 W/cm^2. But CE has also been reported in metastable barium vapor under off-resonant cw excitation with only 25 W/cm^2 [10]. Nonetheless, such relatively low intensity used in the barium experiment is about three orders of magnitude higher than the saturation intensity of the excited atomic transition at line center.

Electromagnetically induced transparency (EIT) allows the combination of a strong Kerr nonlinearity and a small linear absorption to be simultaneously experienced by a resonant field interacting with an atomic medium [11]. Nonlinear optics at low light levels has been proposed [12]; giant XPM nonlinearities are possible even at the few-photon level [13], with applications in quantum nondemolition measurement [14], quantum logic gates [15], and quantum state teleportation [16]. Experimental demonstrations of enhancement of an optical Kerr nonlinearity have been reported in multilevel atomic systems [17–19].

In this Brief Report, we predict theoretically the occurrence of CE with weak field excitation in an atomic medium under EIT. We explore the giant nonlinearities an atomic vapor can exhibit under EIT to create a radially varying XPM phase shift on a probe beam. In the far field, a ring structure can be induced on the probe beam transverse profile by a signal beam with an intensity well below saturation level at line center ($I_{\rm sat} \approx 5$ mW/cm^2 for sodium vapor).

Figure 1 shows the atomic model. It consists of an open four-level atom interacting with three cw lasers. Levels $|3\rangle$ and $|4\rangle$ are excited states that naturally decay at rates γ_3 and γ_4, respectively. Level $|1\rangle$ is the ground state and $|2\rangle$ is a metastable state with negligible decay rate ($\gamma_2 \approx 0$); these levels could be, for example, two hyperfine-split states of an alkaline atom. Transitions $|1\rangle \rightarrow |3\rangle$, $|2\rangle \rightarrow |3\rangle$, and $|2\rangle \rightarrow |4\rangle$ are electric-dipole-allowed, while transitions $|1\rangle \rightarrow |2\rangle$ and $|3\rangle \rightarrow |4\rangle$ are electric-dipole-forbidden. Levels $|1\rangle$ and $|3\rangle$ are connected by a probe beam with Rabi frequency $\Omega_p = 2d_{13}E_p/\hbar$ and wavelength λ, while the $|2\rangle \rightarrow |3\rangle$ transition is driven by a coupling beam (Rabi frequency $\Omega_c = 2d_{23}E_c/\hbar$). Both coupling and probe beams are resonant with their respective transitions, and EIT of the probe beam occurs if $\Omega_c \gg \Omega_p$ [11]. The signal beam ($\Omega = 2d_{24}E_s/\hbar$) is detuned from the $|2\rangle \rightarrow |4\rangle$ transition by $\delta = \omega_{24} - \omega$, where ω_{24} is the atomic transition frequency and ω is the signal optical frequency. The role of the signal field is to create an ac-Stark shift of state $|2\rangle$, causing a large change in the index of refraction at the probe frequency. Giant nonlinearities are induced while keeping the linear susceptibilities identically zero for all fields [13].

The equations of motion for the probability amplitudes of the atomic states are written as

$$\begin{aligned} \dot{a}_1 &= \tfrac{1}{2}i\Omega_p a_3, \\ \dot{a}_2 &= \tfrac{1}{2}i\Omega_c a_3 + \tfrac{1}{2}i\Omega a_4, \\ \dot{a}_3 &= -\Gamma_3 a_3 + \tfrac{1}{2}i\Omega_p a_1 + \tfrac{1}{2}i\Omega_c a_2, \\ \dot{a}_4 &= -\Gamma_4 a_4 + \tfrac{1}{2}i\Omega a_2, \end{aligned} \tag{1}$$

where $\Gamma_3 = \gamma_3/2$ and $\Gamma_4 = \gamma_4/2 + i\delta$. Using the rotating-wave approximation, we solve Eqs. (1) in the steady-state regime. The probe Rabi frequency is assumed to be very small, such that $a_1 \approx 1$.

The induced atomic polarization at the probe frequency is $P_{13} = Nd_{13}a_1^* a_3$, where N is the atomic density. Writing $P_{13} = \epsilon_0 \chi E_p$, where χ is the atomic susceptibility and E_p is the probe's electric-field amplitude, we find

$$\begin{aligned} \mathrm{Re}(\chi) &= \left(2Nd_{13}^2/\hbar\epsilon_0\right)\frac{2(\Omega/\Omega_c)^2\delta}{4\delta^2 + [\gamma_4 + \gamma_3(\Omega/\Omega_c)^2]^2}, \\ \mathrm{Im}(\chi) &= \left(2Nd_{13}^2/\hbar\epsilon_0\right)\frac{\gamma_4(\Omega/\Omega_c)^2 + \gamma_3(\Omega/\Omega_c)^4}{4\delta^2 + [\gamma_4 + \gamma_3(\Omega/\Omega_c)^2]^2}. \end{aligned} \tag{2}$$

*araujo@ifi.unicamp.br

 ©2010 The American Physical Society

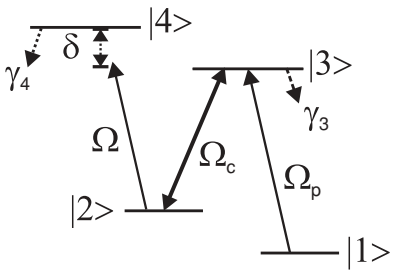

FIG. 1. An illustration of the atomic model: An open four-level atom interacting with three laser beams: probe (Ω_p), coupling (Ω_c), and signal (Ω). $|1\rangle$ is the ground state. The excited $|3\rangle$ and $|4\rangle$ states have a natural decay rate of γ_3 and γ_4, respectively. State $|2\rangle$ is metastable ($\gamma_2 \approx 0$). Throughout our discussion, we will consider typical atomic parameters for the D2 line of Na at $\lambda = 589$ nm: $\gamma_4 \approx \gamma_3 = 2\pi \times 10$ MHz.

In deriving Eqs. (2), no approximations were made with respect to the magnitude of Ω, Ω_c, or Δ. To present our results in a unitless form, we define $R = \Omega/\Omega_c$, $\Gamma = \gamma_4/\gamma_3$, and $\Delta = \delta/\gamma_3$. In the limit that $\Delta \gg \Gamma, R$, Eqs. (2) can be simplified to

$$\begin{aligned} \mathrm{Re}(\chi) &= K\frac{R^2}{2\Delta}, \\ \mathrm{Im}(\chi) &= K\frac{\Gamma R^2 + R^4}{4\Delta^2}, \end{aligned} \tag{3}$$

where $K = 2Nd_{13}^2/\hbar\epsilon_0\gamma_3$. In the absence of the signal field ($R = 0$), the atomic susceptibility χ is null since the coupling field renders the atom transparent to the probe field.

Suppose the probe beam propagates along the z direction and enters an extended atomic medium of length L at $z = 0$. The incident probe field will be assumed to be a plane wave with a Gaussian intensity profile: $E_p(z = 0, \rho, t) = E_0(\rho)\exp[i(k_p z - \omega t)]$, with

$$E_0(\rho) = E_p^0 \exp(-\rho^2/a^2); \tag{4}$$

E_p^0 is the input probe amplitude and a is the beam diameter. We assume that the coupling field has either a uniform transverse profile or a beam diameter much larger than the probe diameter. The probe propagation through the atomic sample is described by Maxwell's wave equation with the atomic polarization as the driving source. In the slowly varying envelope approximation,

$$-i\frac{1}{2k_p}\nabla_T^2 E_p + \frac{\partial E_p}{\partial z} = i\frac{k_p}{2\epsilon_0}P_{13}, \tag{5}$$

where ∇_T is the transverse gradient, $k_p = 2\pi/\lambda$ is the probe wave number, $E_p \equiv E_p(z,\rho)$, and $P_{13} \equiv P_{13}(z,\rho)$. To simplify the notation, we choose the probe diameter a as the unit for the radial coordinate ρ, and z_0 as the unit for the longitudinal coordinate z, where $z_0 = \hbar\epsilon_0\lambda\gamma_3/4\pi N d_{13}^2$ is the probe's one-photon absorption length in the absence of the coupling field. Therefore, in a unitless form, the wave equation becomes

$$-i\frac{1}{\mathcal{N}}\nabla_T^2 E_p + \frac{\partial E_p}{\partial z} = (-\alpha/2 + i\sigma)E_p, \tag{6}$$

where $\alpha = (\Gamma R^2 + R^4)/4\Delta^2$ is the nonlinear-absorption coefficient, $\sigma = R^2/2\Delta$ is the XPM phase shift of the probe laser per absorption length, and $\mathcal{N} = 4\pi a^2/\lambda z_0$ is the beam Fresnel number.

The transverse term can be eliminated from Eq. (8) if $\mathcal{N} \gg 1$. For a probe diameter of $a = 1$ mm, $\gamma_3/2\pi = 10$ MHz, $N \lesssim 10^{12}$ cm^{-3}, and $d_{13} = 1.2 \times 10^{-29}$ Cm, then $\mathcal{N} \approx 1500$. Under this condition, diffraction of the probe beam within the sample can be neglected, and its propagation is described by

$$\frac{\partial E_p}{\partial z} = (-\alpha/2 + i\sigma)E_p. \tag{7}$$

Equation (7) is readily solved to find the probe field at the exit plane $z = \ell = L/z_0$ of the atomic medium,

$$E_p(\rho) = E_0(\rho)\exp(-\alpha\ell/2 + i\phi). \tag{8}$$

As the probe beam traverses the atomic sample, it acquires a phase $\phi = \sigma\ell$ from the signal beam through XPM. In the limit that $R \ll 1$, a large XPM phase shift can be induced on the probe beam with an arbitrarily weak signal field over long interaction lengths, such as those found in atomic vapor cells. The scheme is limited by the small nonlinear absorption given by α [13]. Over short interactions lengths, consistent with magneto-optical traps, a large XPM phase can also be obtained for $R \gtrsim 1$, at the expense of a larger signal detuning to keep probe absorption low. If the ground-state decoherence rate is negligible ($\gamma_2 \approx 0$), both signal and coupling beams can still be weak.

If the signal beam, propagating collinear with the probe beam, also has a Gaussian profile of identical width to the probe beam, then the XPM probe phase will be

$$\phi = \phi(\rho) = \phi_0 e^{-2\rho^2}, \tag{9}$$

where $\phi_0 = R^2\ell/2\Delta$. Therefore, the signal beam induces a probe phase shift that varies with the transverse distance ρ from the probe beam's axis. The maximum XPM phase shift ϕ_0 imparted to the probe field depends on three parameters: the signal-to-coupling Rabi-frequency ratio R, the signal detuning Δ, and the length ℓ of the atomic medium. In modulus, the phase shift is the same for positive and negative signal detunings of equal magnitudes.

The far-field diffraction pattern of the transmitted probe beam is found by taking a two-dimensional (2D) Fourier transform of the probe field at the exit plane. Due to the cylindrical symmetry of the problem, the 2D Fourier transform reduces to a zeroth-order Hankel transform. The far-field intensity distribution of the probe beam, on an observation plane at a distance D away from the sample, is given by

$$I(k_r a) \propto \left| \int_0^\infty E_0(\rho) e^{[-\alpha(\rho)\ell/2 + i\phi(\rho)]} J_0(k_r a\rho)\rho\, d\rho \right|^2, \tag{10}$$

where $k_r = k_p a r/D$ is the radial wave number, with r being the radial coordinate in the observation plane (in units of a); J_0 is the zeroth-order Bessel function. Diffracted fields from distinct regions of overlap between pump-and-probe beams can interfere with each other if they have the same wave vector. The interference, which can be either constructive or destructive, produces multiple concentric rings in the far-field region. The number of rings is approximately $\phi_0/2\pi$ [3]. The

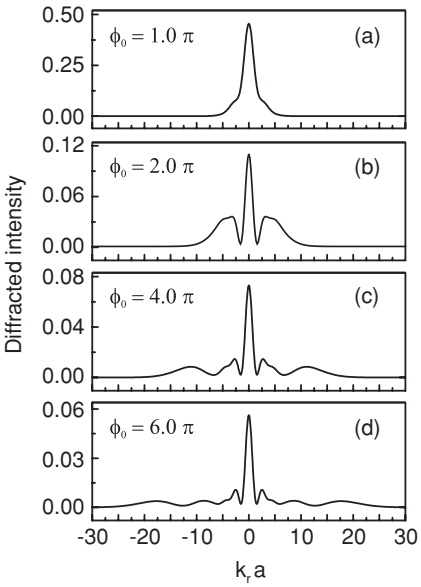

FIG. 2. Far-field diffraction pattern of the probe beam after traversing an atomic medium of length (a) $\ell = 33$, (b) $\ell = 65$, (c) $\ell = 130$, and (d) $\ell = 190$. The peak XPM phase shift ϕ_0 is also shown for each case. Here, $R = 4$, $\Delta = 80$, and $\Gamma = 1$. The diffraction intensity is normalized as described in the text.

generated rings are of the same optical frequency as the original probe beam.

Figure 2 shows the transverse spatial profile of the diffracted probe beam for various interaction lengths ℓ inside the atomic sample. All curves are normalized with respect to the intensity at $r = 0$ with the nonlinear phase set to $\phi \equiv 0$. The peak phase ϕ_0 for each ℓ is also indicated. As the interaction length increases, the XPM phase increases, and along with it, the number of CE rings. For $\ell = 33$, the XPM phase shift is less than 2π and a ring structure has not started to form yet, although a small pedestal can be seen. But at $\ell = 65$ ($\phi_0 = 1.0 \times 2\pi$), a single ring forms around the probe beam's axis. For $\ell = 130$, the peak XPM phase shift is $\phi_0 = 2.0 \times 2\pi$, and a second ring is visible. At $\ell = 190$, for which $\phi_0 = 3.0 \times 2\pi$, a third ring can be seen. While the diameter of the first ring remains approximately constant, that of the outermost ring increases linearly with the propagation distance.

The diameter of the outermost ring is directly related to its half-cone angle θ, which is estimated by [3]

$$\theta \approx \frac{1}{k_p}\left|\frac{d\phi}{d\rho}\right|_{\max}. \tag{11}$$

From Eq. (9), we find

$$\theta \propto \ell R^2/|\Delta|. \tag{12}$$

We see that the cone angle is linearly proportional to the propagation length ℓ, as observed in Fig. 2, and proportional to the square of the signal-to-coupling Rabi-frequency ratio R. Since $\ell = L/z_0 \propto N$, the cone angle varies linearly with atomic density. CE as a result of self-modulation also exhibits a linear dependence of the cone angle with N [4], while for CE from four-wave mixing, $\theta \propto N^{0.5}$ [9], and from the cooperative effect, $\theta \propto N^2$ [8]. CE occurs for both red- and blue-detuned signal fields, and the cone angle is inversely proportional to the signal detuning.

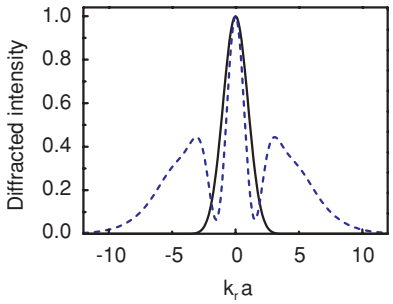

FIG. 3. (Color online) Diffracted intensity distribution with (dashed blue line) and without (solid black line) XPM.

Much like the XMP phase ϕ, the nonlinear absorption coefficient is also radially varying: $\alpha(\rho) = (\Gamma R^2 e^{-2\rho^2} + R^4 e^{-4\rho^2})/4\Delta^2$. To verify that the CE patterns result from the XPM phase shift induced on the probe field by the signal field, we artificially set $\phi(\rho) \equiv 0$, but keep the radial dependence of the absorption coefficient $\alpha(\rho)$ in Eq. (10). The diffraction patterns with and without the XPM phase are shown in Fig. 3. In both cases, $R = 4$, $\Delta = 80$, $\ell = 60$, and $\Gamma = 1$, under which conditions $\alpha(0)\ell = 0.63$, corresponding to a 53% probe transmission at its axis. (Without EIT, the probe transmission would be negligible: e^{-60}.) Here, the intensity patterns are normalized by their peak intensities for better viewing and comparison of the two curves. Without XPM, no ring structure is seen in the far-field intensity distribution, confirming that XPM is the main mechanism responsible for CE in our scheme.

Except for the particular form of the $\exp[-\alpha(\rho)\ell/2]$ term, Eq. (10) is quite general and describes the far-field diffraction pattern observed under any physical mechanism that induces a change of the sample's refractive index proportional to the light intensity in the sample. The far-field patterns shown here resemble those observed under self-phase modulation of a strong pump beam, for example [2]. The most interesting part of our work is the physical mechanism responsible for CE: a giant XPM phase shift of a weak probe beam induced by a weak signal field.

We next estimate the necessary Rabi frequencies to observe CE under the present scheme. In a homogeneously broadened atomic vapor, EIT occurs for $\Omega_c^2 > \gamma_2\gamma_3$, which sets the required lower limit for the coupling Rabi frequency. Typically, in a magneto-optical trap, for example, $\gamma_2/2\pi \approx 1$ kHz [17]; for $\gamma_3/2\pi = 10$ MHz, one must have $\Omega_c/2\pi > 100$ kHz. For a hot atomic sample, the EIT condition is $\Omega_c^2 \gg (\gamma_2/\gamma_3)\Delta_D^2$ [20], where $\Delta_D/2\pi \approx 500$ MHz is the typical, inhomogeneously broadened Doppler width found in many EIT experiments with hot atoms; in a vapor cell with buffer gas and large beams, it is possible to achieve $\gamma_2/2\pi \approx 100$ Hz [21]. Therefore, $\Omega_c/2\pi \gg 16$ kHz for EIT to occur. In our discussion, we considered an excitation regime in which $\Omega \gtrsim \Omega_c \gg \Omega_p$. Hence, a Kerr nonlinearity large enough to cause CE of the probe beam can be obtained with signal, coupling, and probe Rabi frequencies well below saturation levels ($\Omega, \Omega_c, \Omega_p < \gamma_3$) in both hot and cold atomic samples. For sodium vapor, these Rabi frequencies would correspond to intensities below

5 mW/cm^2. To the best of our knowledge, the estimated light levels for observing CE in the current scheme are several orders of magnitudes lower than those required in all the CE schemes studied so far.

To observe CE under the proposed scheme, the required optical depths are easily obtainable in a vapor cell, although precise predictions would require introducing an inhomogeneous Doppler broadening into the model. The cold-atom case poses an experimental challenge in that the optical depths to develop the necessary XPM phase shifts are fairly large. But optical depths as large as 160 have been reported for a Na "dark-spot" magneto-optical trap [22] and optical depths of 105 have been demonstrated in cigar-shaped Cs atom clouds [23]. Figure 2(b) shows that an optical depth of 65 is sufficient to observe the formation of a single CE ring. So CE under the conditions studied here should be observable with existing technology.

In conclusion, we proposed a scheme under which conical emission can be observed in an atomic vapor excited at low light levels. Exploiting the large XPM phase shifts afforded by EIT, diffraction rings can be induced on a probe beam by a signal field with an intensity below the saturation intensity of an atomic transition.

The authors acknowledge the financial support of INOF-CNPq and FAPESP.

[1] R. W. Boyd, *Nonlinear Optics* (Academic, San Diego, 1992).
[2] *Self-focusing: Past and Present: Fundamentals and Prospects*, edited by R. W. Boyd, S. G. Lukishova, and Y. R. Shen (Springer, New York, 2009).
[3] S. D. Durbin, S. M. Arakelian, and Y. R. Shen, Opt. Lett. **6**, 411 (1981).
[4] M. L. Ter-Mikaelian, G. A. Torossian, and G. G. Grigoryan, Opt. Commun. **119**, 56 (1995).
[5] W.-K. Lee *et al.*, J. Opt. Soc. Am. B **18**, 101 (2001).
[6] V. Pilla, L. de S. Menezes, M. A. R. C. Alencar, and C. B. de Araújo, J. Opt. Soc. Am. B **20**, 1269 (2003).
[7] L. You, J. Mostowski, J. Cooper, and R. Shuker, Phys. Rev. A **44**, R6998 (1991).
[8] Y. Ben-Aryeh, Phys. Rev. A **56**, 854 (1997).
[9] D. J. Harter and R. W. Boyd, Opt. Lett. **7**, 491 (1982).
[10] G. De Filippo, S. Guldberg-Kjaer, S. Milosevic, and J. O. P. Pedersen, Opt. Commun. **144**, 315 (1997).
[11] M. Fleischhauer, A. Imamoglu, and J. P. Marangos, Rev. Mod. Phys. **77**, 633 (2005).
[12] S. E. Harris and L. V. Hau, Phys. Rev. Lett. **82**, 4611 (1999).
[13] H. Schmidt and A. Imamoglu, Opt. Lett. **21**, 1936 (1996).
[14] A. D. Greentree, R. G. Beausoleil, and L. C. L. Hollenberg, New J. Phys. **11**, 093005 (2009).
[15] Q. A. Turchette, C. J. Hood, W. Lange, H. Mabuchi, and H. J. Kimble, Phys. Rev. Lett. **75**, 4710 (1995).
[16] D. Vitali, M. Fortunato, and P. Tombesi, Phys. Rev. Lett. **85**, 445 (2000).
[17] H. Kang and Y. Zhu, Phys. Rev. Lett. **91**, 093601 (2003).
[18] A. B. Matsko, I. Novikova, G. R. Welch, and M. S. Zubairy, Opt. Lett. **28**, 96 (2003).
[19] S. Li *et al.*, Phys. Rev. Lett. **101**, 073602 (2008).
[20] A. Javan, O. Kocharovskaya, H. Lee, and M. O. Scully, Phys. Rev. A **66**, 013805 (2002).
[21] M. Erhard and H. Helm, Phys. Rev. A **63**, 043813 (2001).
[22] W. Ketterle, K. B. Davis, M. A. Joffe, A. Martin, and D. E. Pritchard, Phys. Rev. Lett. **70**, 2253 (1993).
[23] Y.-W. Lin *et al.*, Opt. Express **16**, 3753 (2008).